SunShot
U.S. Department of Energy

CSP Program Summit 2016

High Temperature Molten Salt Corrosion in CSP Systems

Savannah River National Laboratory
University of South Carolina
University of Alabama

Brenda L. Garcia-Diaz, Josh R. Gray, Luke C. Olson, Michael J. Martinez-Rodriguez, Roderick E. Fuentes, Sirivatch Shimpalee, Ramana G. Reddy, and John W. Van Zee

Overview

Info & Timeline

Funding Opportunity: SunShot Lab Call
Project Identifier: Garcia-Diaz_A
PI: Brenda L. Garcia-Diaz

- Project Start Date: 10/01/12
- Project End Date: 12/31/16
- Percentage Completion: 98%

Barriers

- CSP Plant Operation with Advanced Power Cycles (T>700°C)
- System lifetime > 30 years
- Cost of Power < $0.06 / kWh

Budget

Total Project Budget: $3,850,000

- Total Recipient Share: $3,850,000
- Total Federal Share: $3,850,000
- Total DOE Funds Spent: $3,800,000

* As of 3/31/16

Partners

- SRNL (Lead)
- University of Alabama
- University of South Carolina
- Haynes International

Objectives

- Characterize corrosion in CSP systems operating above 700°C with molten salts
- Model corrosion mechanisms and kinetics
- Measure corrosion rates and compare with service lifetime goals for a variety of heat transfer system materials
  - 30 year lifetime SunShot corrosion rate target is $< 15\ \mu m/yr$
- Identify and characterize methods to prevent corrosion in molten salt CSP systems

Problem Statement and Value Proposition

- SunShot program seeks major price reductions
- Higher temperature energy conversion allows for better thermodynamic efficiencies
- Temp. Range for Study: 800 – 1000 °C
- Limited number of options for very high temperature heat transfer
  - Steam or other gases
    - *Large pipe diameters needed*
    - *Large pumping power required*
  - Molten Glass
    - *Viscous*
    - *Low thermal conductivities*
  - Liquid metals
    - *Limited operating temperature range*
    - *Alloying with piping materials*
    - *Vapor pressures*
  - Molten Salts
    - *Heat transfer behavior at 700 °C similar to water at 20 °C*

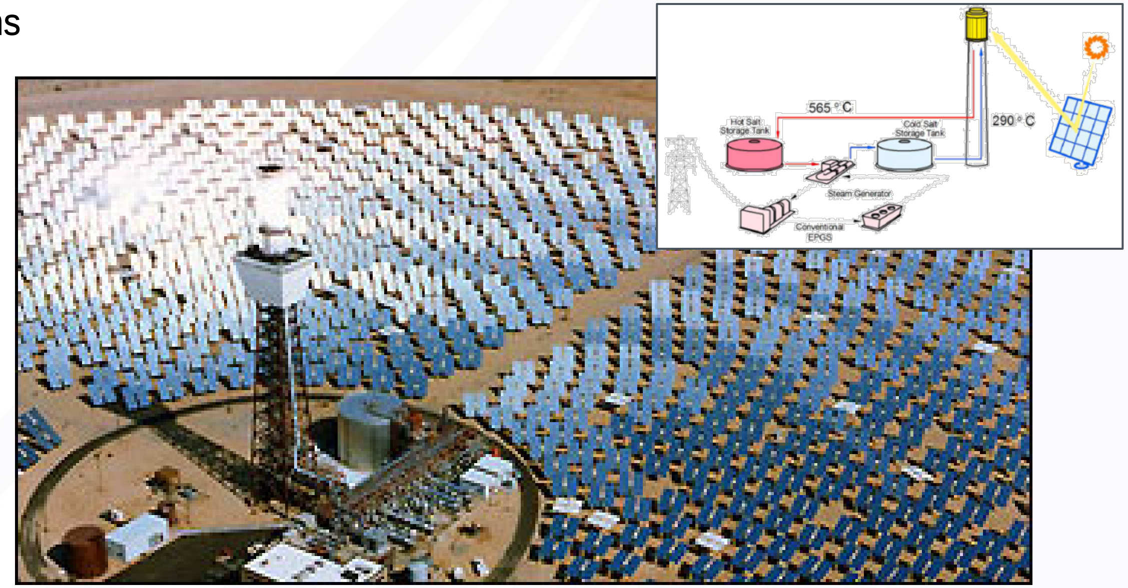

Image Source: NREL, available: http://earthobservatory.nasa.gov/Features/RenewableEnergy/Images/solar_two.jpg
Table Source: SAND2011-2419

Table 5. Cost of steam generator subsystem [$/kW$_e$] expressed in 2010 dollars

Steam Generator System Component	Utility Studies 100 MW_e (260 MW_t)	Abengoa Study 400 MW_e (1000 MW_t)	Roadmap Workshop Baseline
Heat Exchangers	214	110	–
Structures/Foundations	1	0.5	–
Piping	22	12	–
Hot Salt Pumps	10	12	–
Auxiliary Equipment	3	2	–
Spare Parts and Other Directs	1	9	–
Contingency	38	22	–
Total Capital Cost	**$290/kW$_e$**	**$168/kW$_e$**	**$250/kW$_e$**

High Temperature Molten Salt Corrosion Testing

- Identify molten salt/material combinations that have long service life and meet performance needs
- Characterize corrosion rates, corrosion mechanisms, and methods to reduce corrosion
- Long-term and electrochemical testing
- Quartz or Inconel 625 vessels with water cooled flanges and machined electrode pass-throughs
- Reference electrodes
  - Ag/AgCl for chloride, Ni/NiF_2 for fluoride
- Samples: flats, U-bends, and welded

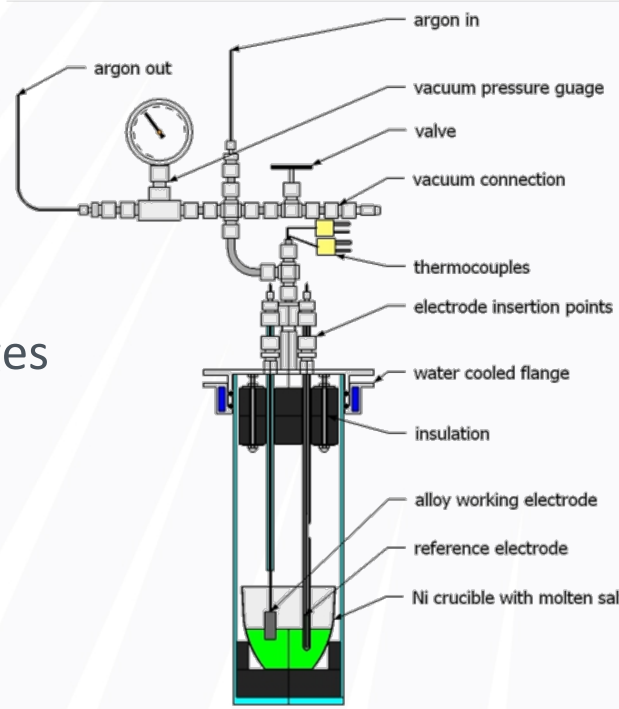

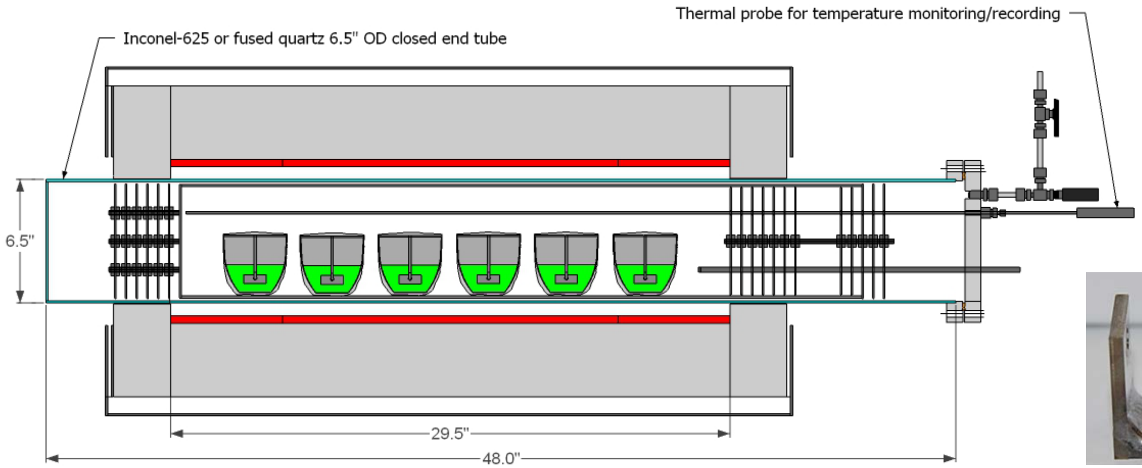

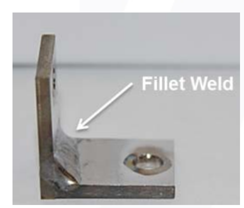

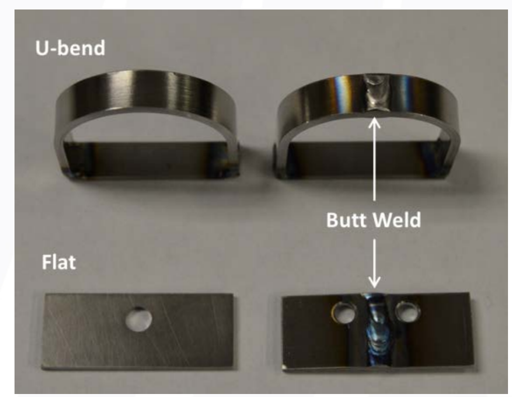

Accelerated Corrosion Results – Electrochemical Analysis

(Haynes 230 in $MgCl_2$-KCl at 850°C)

- CVs give a qualitative map of the EC reactions occurring on the coupon surface.

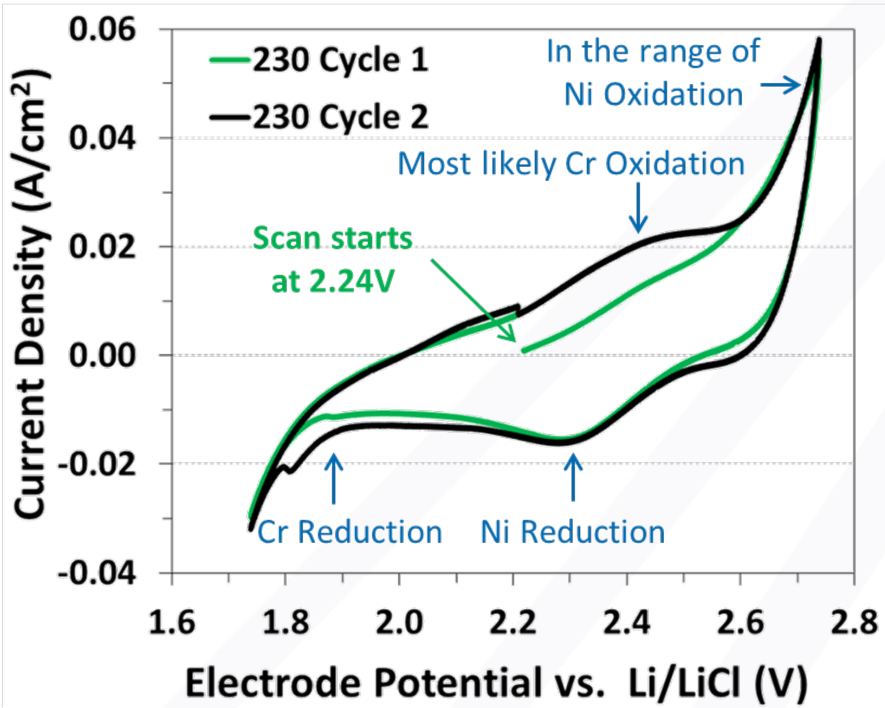

- EIS performed at E_{corr} and under load to characterize corrosion mechanisms and corrosion rates.

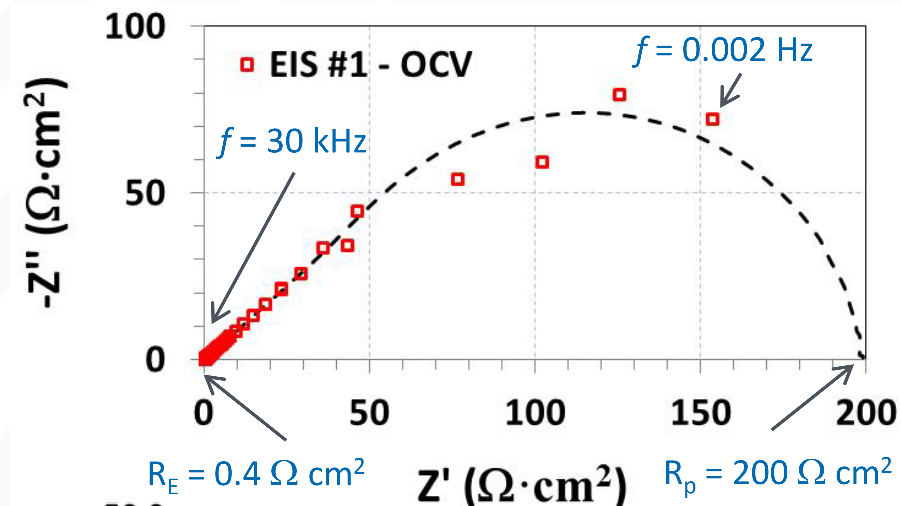

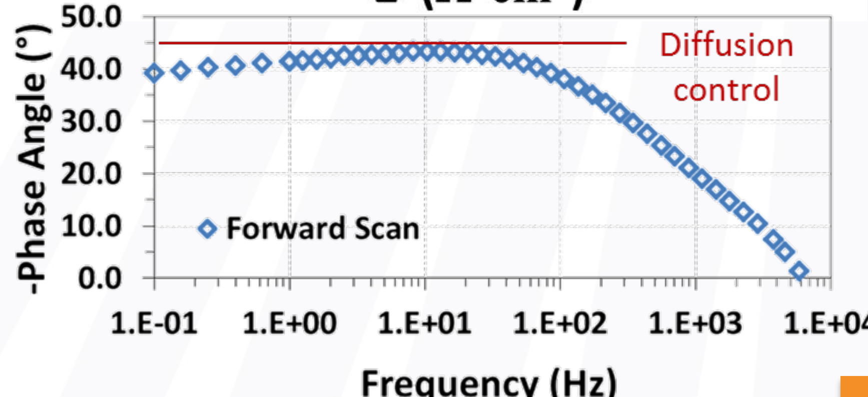

Fe-Ni-Cr Alloy Cyclopoteniodynamic Polarization
($MgCl_2$-KCl at 850°C)

- CPP scans were performed
  - As a normal measurement of the polarization behavior of the electrodes (forward scan)
  - As a characterization of the susceptibility of the sample to localized corrosion (reverse scan)
- Conventional Fe-Ni-Cr alloys (Cr content 22–27%) show corrosion rates that are relatively high and could only be used when employing corrosion inhibition methods
- Incoloy 800H shows the highest general corrosion rate and no localized corrosion

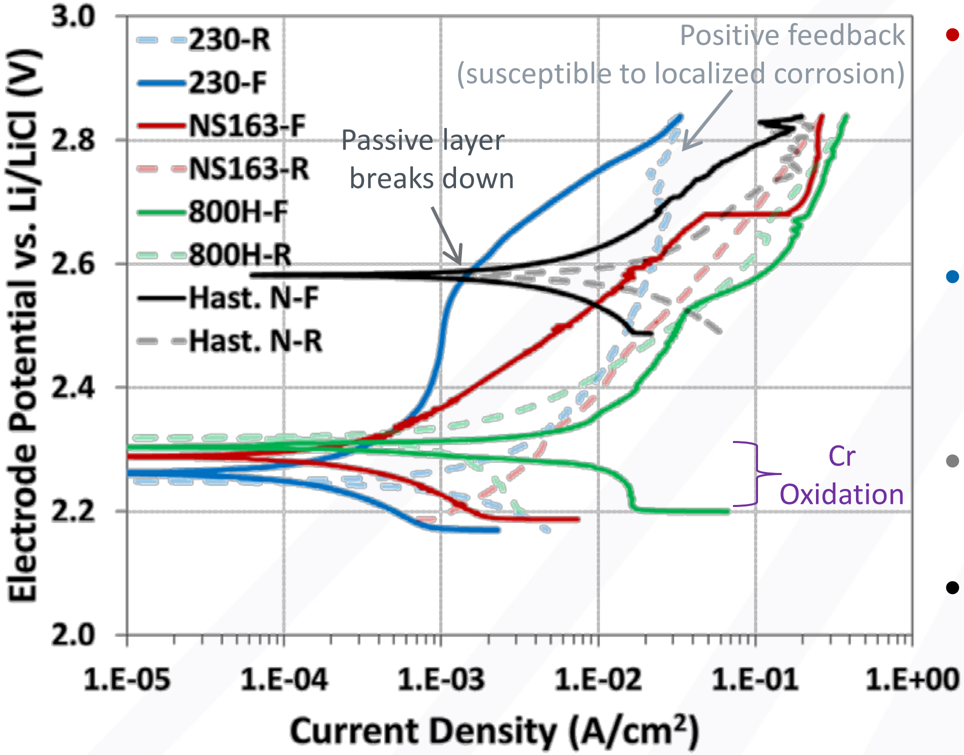

- Haynes NS163 shows 2nd highest general corrosion despite being a Co based alloy and localized corrosion. It has significant amount of Fe relative to Haynes 230
- Haynes 230 show lowest corrosion with passivation until Ni oxidized (passive layer breaks down)
- Hastelloy N has higher E_{corr} due to low Cr, but high general corrosion likely due to Fe content
- All alloys, except Hastelloy N, have corrosion potentials between 2.26 and 2.31 V where Cr oxidation occurs

Long Term Isothermal Performance Qualification

- Arrhenius plots have been constructed which can be used to extract the activation energy for each alloy
- This information can be used in the theoretical analysis to help predict the response of boundary conditions as a function of temperature
- By comparing these activation energies with other literature data, it was seen that the diffusion coefficients were most representative of diffusion along grain boundaries in alloys.

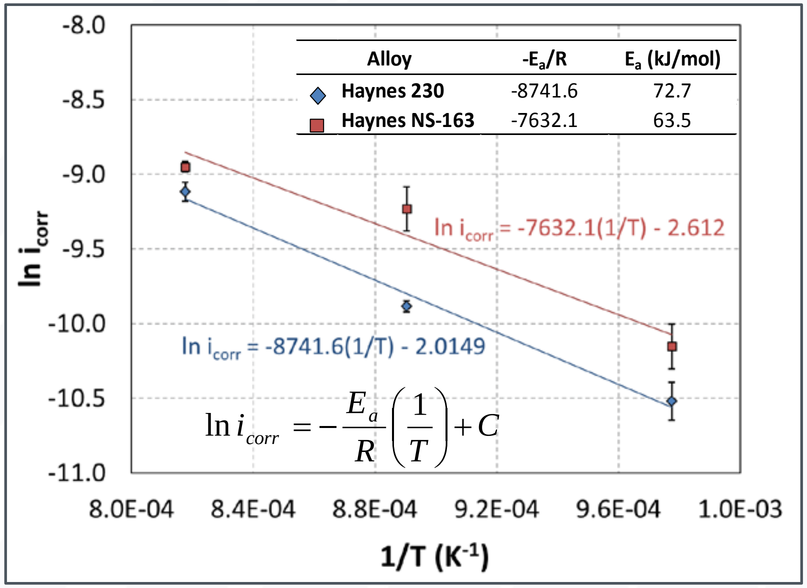

Metal/Alloy	Temperature (°C)	Activation Energy (kJ/mol): Grain Boundary	Activation Energy (kJ/mol): Lattice	Reference
Ni-Based Alloys	585 - 1151	150 - 350	280 - 340	Chen et al. (2003)
Ni	1100 - 1268		273	Gale (2004)
Ni (in FLiNaK)	600 - 850	120	310	Olson (2009)
SS	245 - 900	85 - 234		Mizouchi et al. (2004)
From Arrhenius Plots				
Haynes 230 (in FLiNaK)	750 - 1000	80		
Haynes NS-163 (in FLiNaK)	750 - 1000	144		
Haynes 230 (in $MgCl_2$-KCl)	750 - 950	73		
Haynes NS-163 (in $MgCl_2$-KCl)	750 - 950	64		

Olson, L. (2004), PhD. Dissertation, Univ. of Wisconsin-Madison
Gale, W.F. & Totemeier, T.C (2004), *Smithells Metals Reference Book,* 8th Ed, Elsevier.
Chen, T. et al. (2003), *Materials Transactions*, **44** (1), 40-46.
Mizouchi, M. (2004), *Materials Transactions*, **45** (10), 2945 to 2950

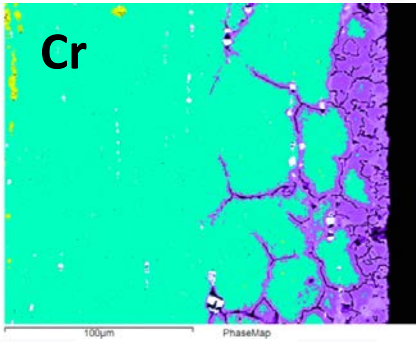

Thermosiphon Corrosion Testing with Flow

- Thermosiphons were designed to provide natural convective flow of the molten salt between a hot section and a cold section
- Design allows corrosion analysis for samples in the hot and cold sections separately
- Large furnaces for heating the thermosiphons are used
- Temperature measurements performed throughout the thermosiphon height in the center and along the edge

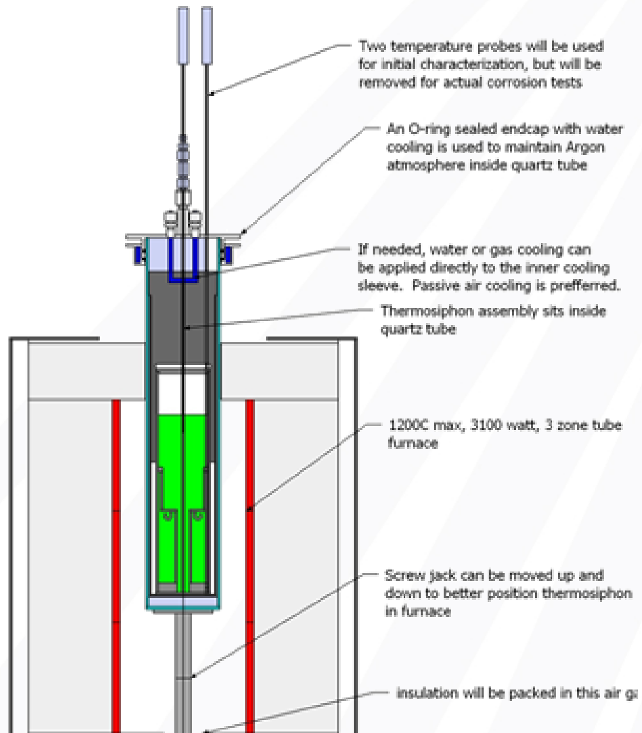

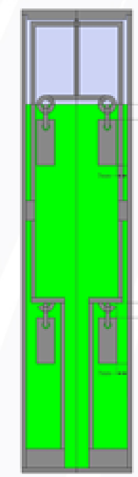

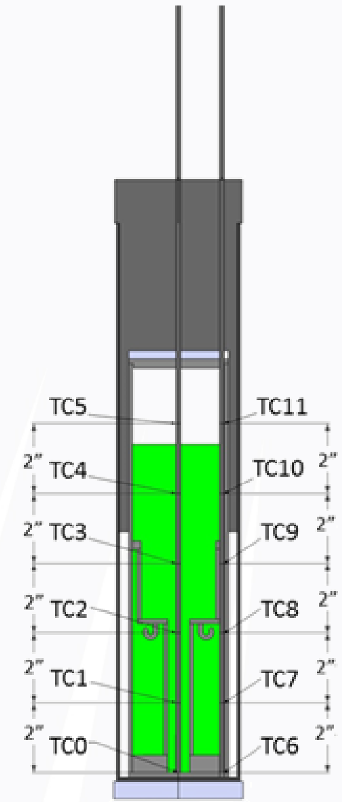

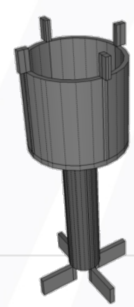

Ni thermosiphon diverter insert

CFD Prediction in the Thermosiphon

Temperature Profiles

- The predictions agree with the experimental data with less than 1% error

800~950°C

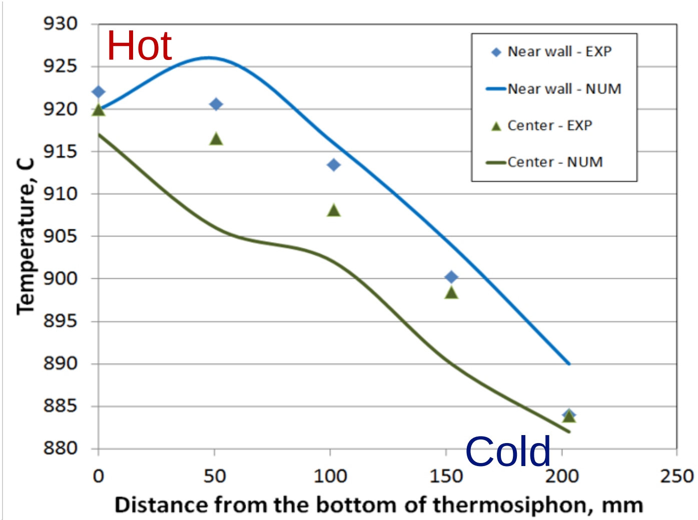

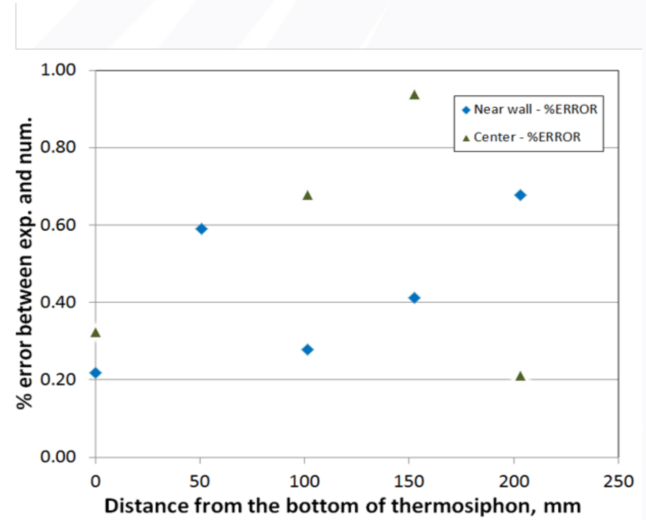

690~800°C

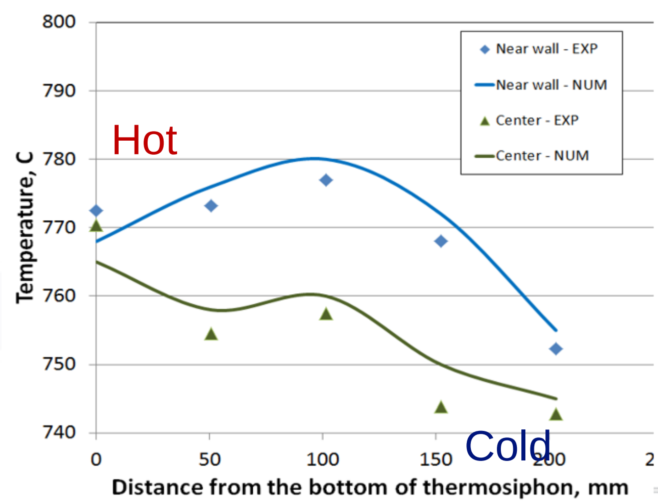

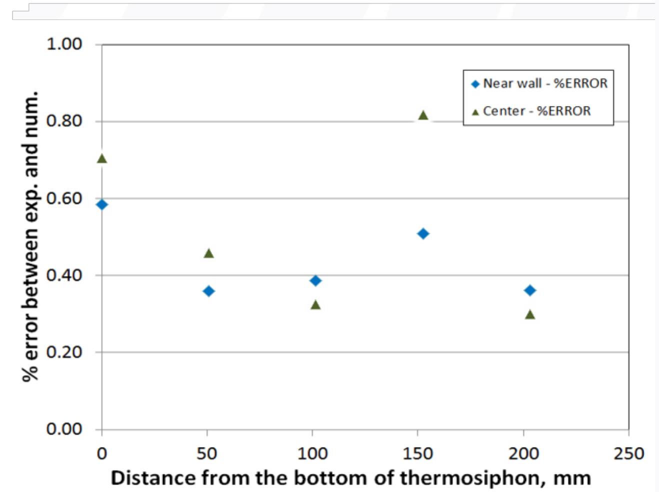

Dimensionless Analysis in the Thermosiphon

- Confirm natural convection flow for the SRNL experimental design
- Gr>>1 (buoyancy force>viscous force), Ra<10^9 (Laminar flow inside of the thermosiphon)

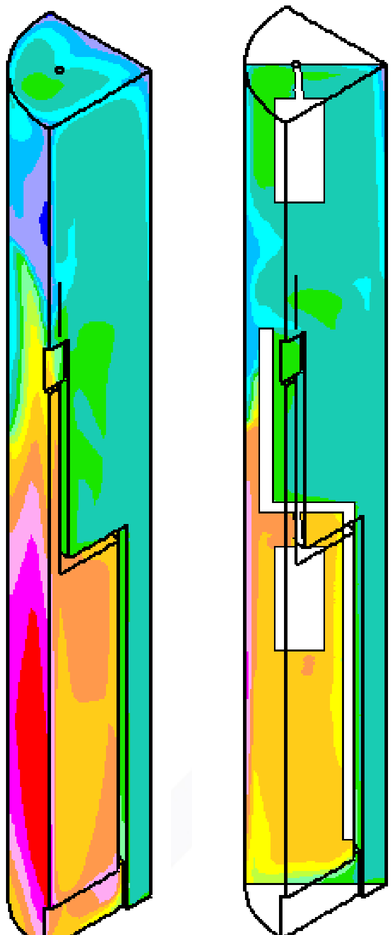

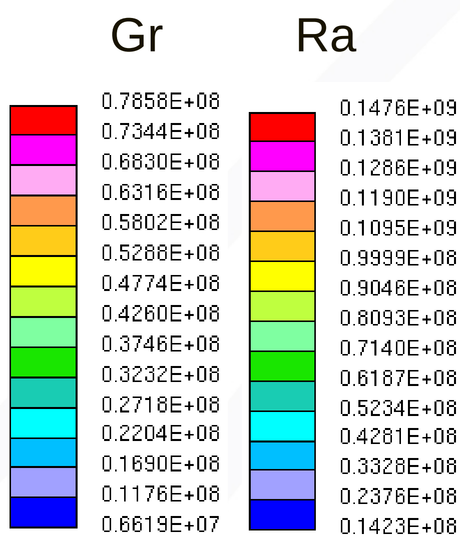

$$Gr = \frac{\text{Buoyancy Forces}}{\text{Viscous Forces}}$$

$$Ra = \frac{\text{Natural Convection}}{\text{Diffusive Mass Transport}}$$

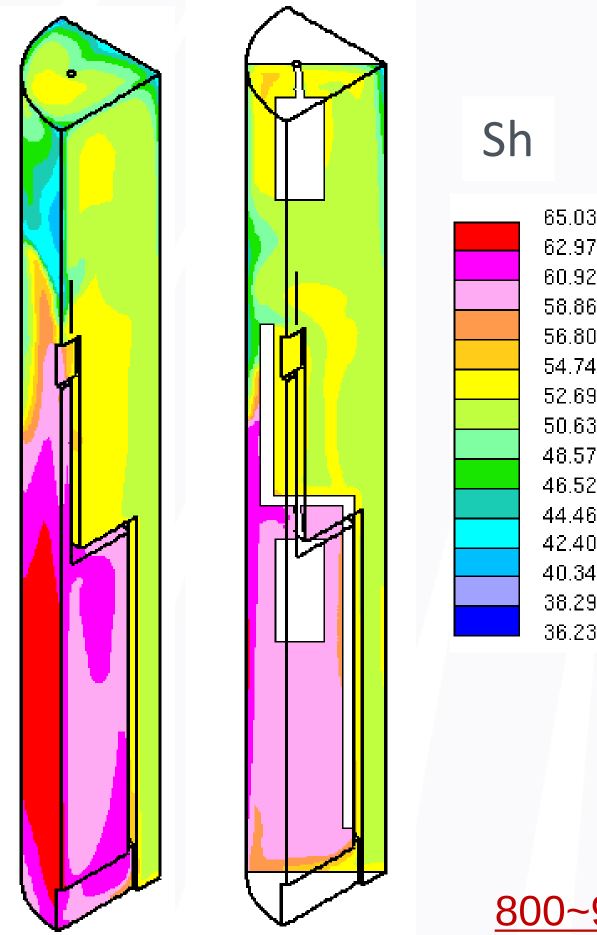

T_∞ = temperature at the top of thermosiphon (T_∞ = 880°C)

800~950°C

Prediction of the Corrosion Rate with Fluid Flows

- Larger Gr & Ra numbers in hot zone due to the bigger ΔT or/and ΔC between outside boundary layer and surface = higher corrosion rate for the coupon in hot zone
- Higher corrosion rates (4-5 times) with fluid flows than the rates without fluid flows

Corrosion rates around the coupons with fluid flows for Haynes 230 in $MgCl_2$-KCl

Cold zone

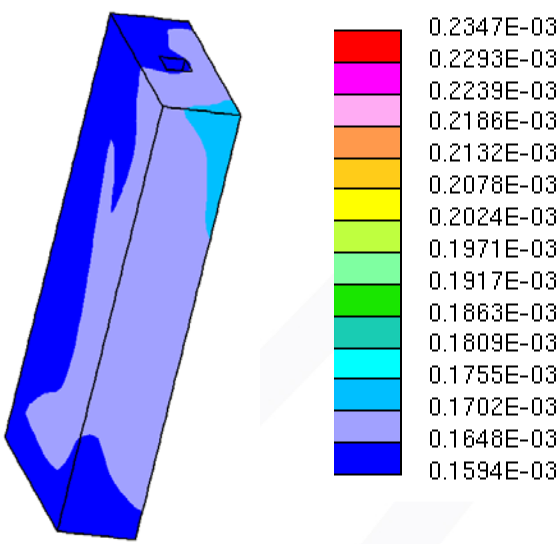

Hot zone

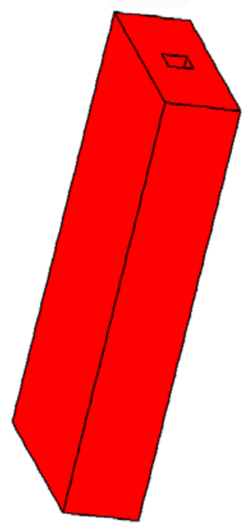

i [A/cm^2]	Cold zone
Numerical	1.64×10^{-4}
Experiments	1.70×10^{-4}

i [A/cm^2]	Hot zone
Numerical	2.33×10^{-4}
Experiments	2.20×10^{-4}

Stagnant @850°C i_{avg}= 0.46 $\times 10^{-4}$ A/cm^2

A case for 800~950°C

Corrosion Testing and Modeling for Haynes 230 in $MgCl_2$-KCl

- CFD simulations were improved so that they did not need to rely on the use of dimensionless numbers for corrosion rate prediction
- The corrosion in isothermal systems without flow and in the thermosiphon systems were both predicted using the CFD model with the same kinetic and mass transfer parameters to within 10%
- Tests showed that experimental results could be predicted for a variety of conditions

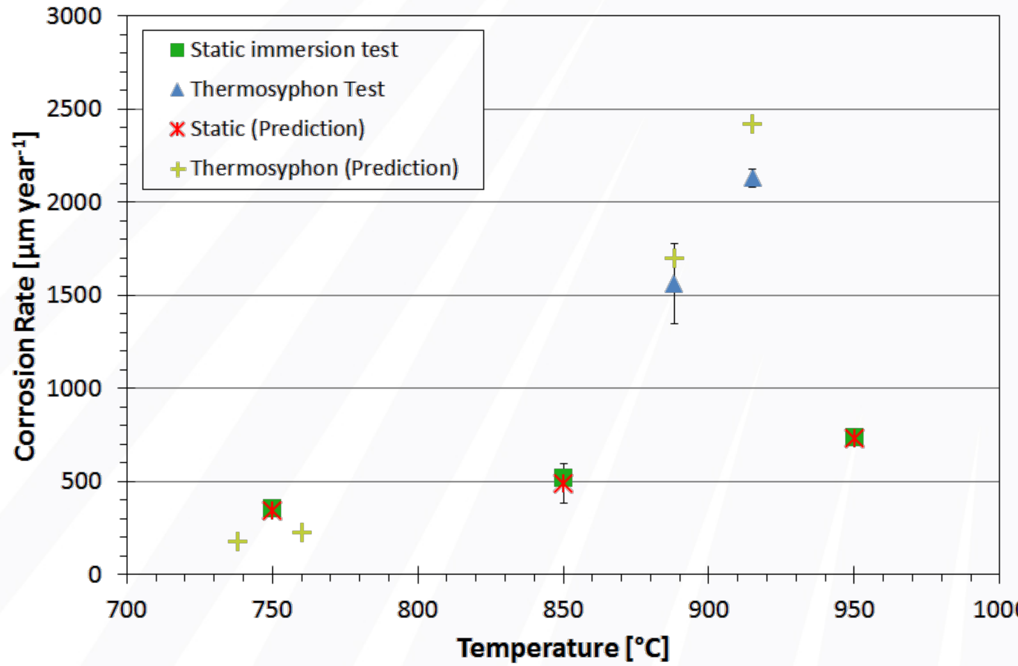

Corrosion Mechanism in $MgCl_2$-KCl

Corrosion initiation step can be caused by impurities such as moisture or oxygen that add a finite concentration of chromium chloride to the salt

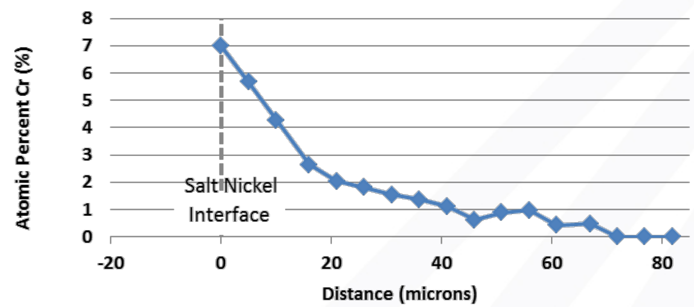

EDS line scan from a cross-section of a Ni crucible containing a single Incoloy-800H coupon

Disproportionation (Crucible)	
Ox :	$2CrCl_2 + 2Cl^- \rightarrow 2CrCl_3 + 2e^-$
Red :	$Ni + CrCl_2 + 2e^- \rightarrow NiCr + 2Cl^-$
Total :	$Ni + 3CrCl_2 \rightarrow NiCr + 2CrCl_3$

Overal Reaction : $Ni + CrCl_3 \leftrightarrow NiCr$

Initiation	
Ox :	$Cr_{23}C_6 + 69Cl^- \leftrightarrow 23CrCl_3 + 6C + 69e^-$
Red :	$34.5MgCl_2 + 34.5H_2O + 69e^- \leftrightarrow 34.5H_{2(g)} + 34.5MgO + 69Cl^-$
Total :	$34.5MgCl_2 + 34.5H_2O + Cr_{23}C_6 \leftrightarrow 34.5H_{2(g)} + 34.5MgO + 23CrCl_3 + 6C$

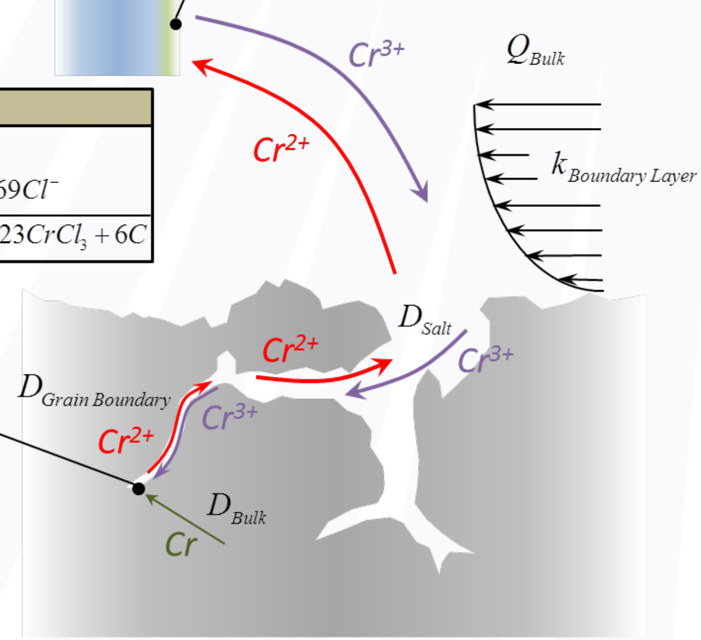

EDS X-ray map of Cr from Haynes 230 cross-section

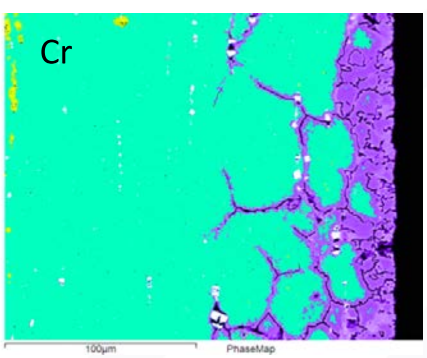

Propagation (Alloy)	
Ox :	$Cr + 2Cl^- \rightarrow CrCl_2 + 2e^-$
Red :	$2CrCl_3 + 2e^- \rightarrow 2CrCl_2 + 2Cl^-$
Total :	$Cr + 2CrCl_3 \rightarrow 3CrCl_2$

Alloy Surface

Corrosion Inhibitor Strategy

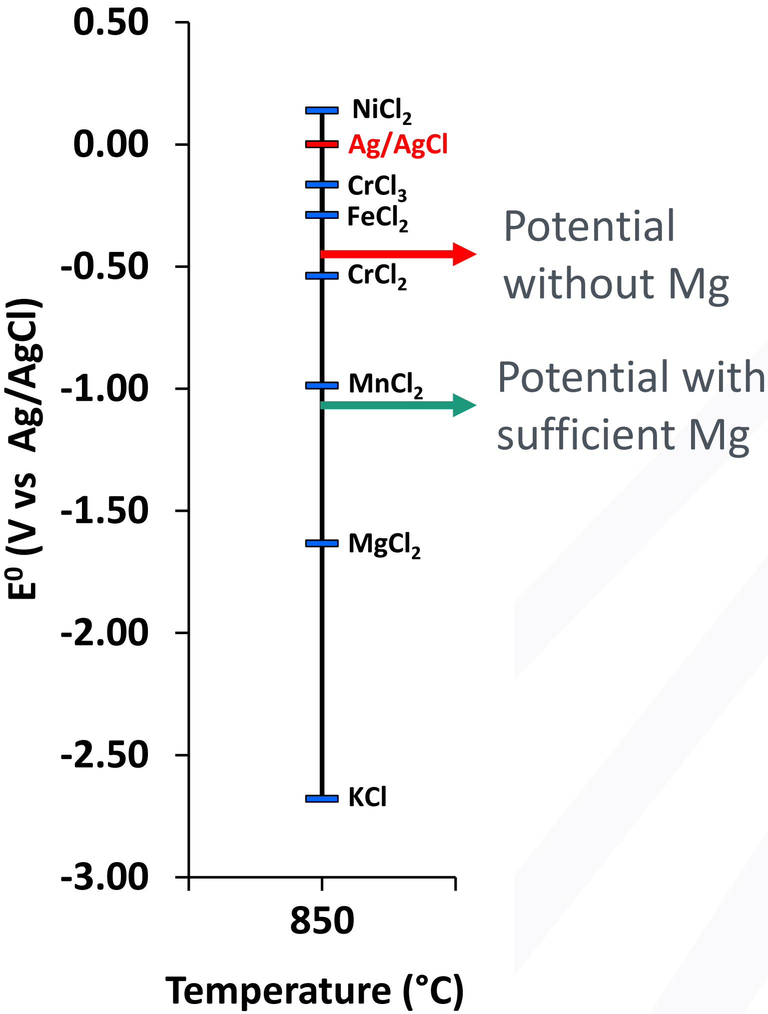

Reaction : $s_O \mathrm{O} + ne^- \rightarrow s_R \mathrm{R}$

Nerst Equation : $E = E^o - \frac{RT}{nF} \ln\left(\Pi a_i^{s_i}\right)$

- Potential without Mg in salt shows Cr can oxidize to $CrCl_2$
- Potential with Mg in salt is well below oxidation potentials for Ni, Fe, and Cr
- Only Mn is close to being oxidized, but is present in small quantities and usually reacts with impurities during alloy formation and is already in an oxidized state
- Therefore, preliminary experiments help explain action of Mg as a sacrificial inhibitor

Monitoring Corrosion Potential with Mg

- Corrosion potential monitoring tests with the commercial salt showed the absolute potential is close to the pure salt with the potential increasing slightly at longer times
- Adding 0.7 mol% Mg to the commercial salt resulted in a corrosion potential below -1.0 V vs Ag/AgCl which indicates the sample is protected from corrosion over the 100 hour test

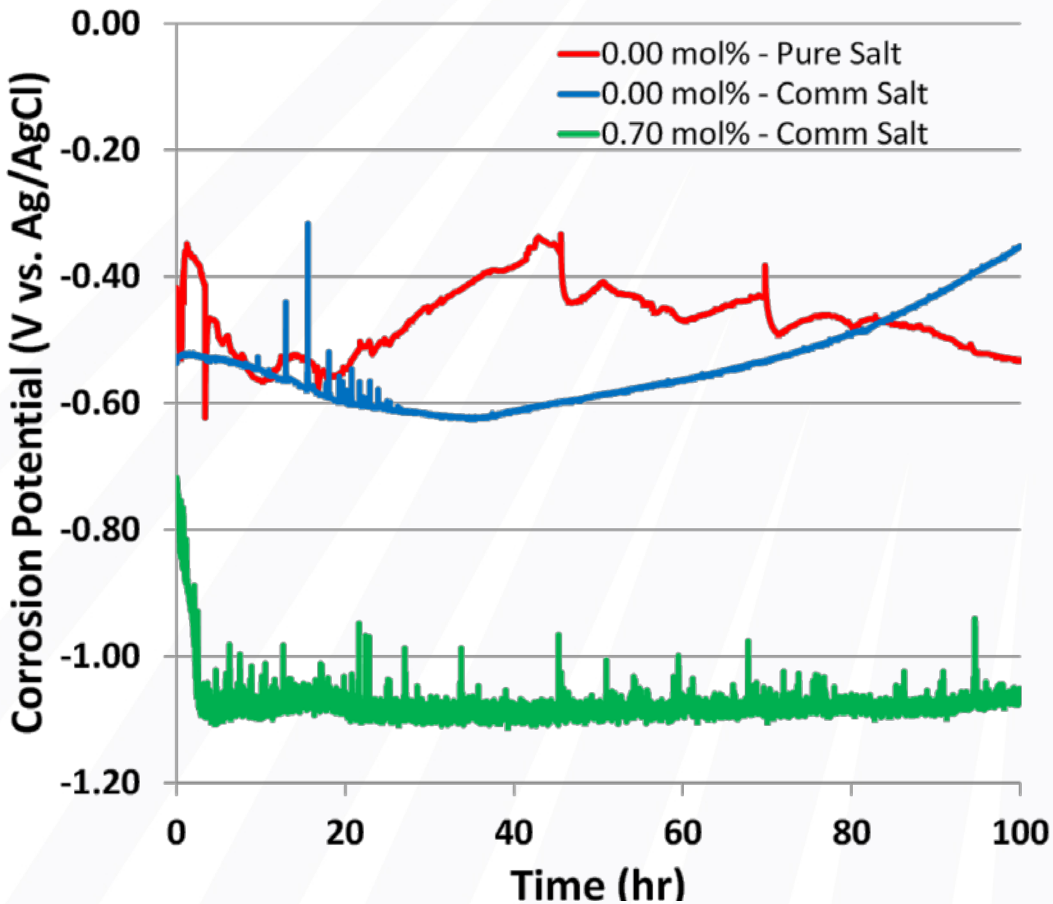

Assessment of Cathodic Protection Effectiveness

- Isothermal corrosion for Haynes 230 in $MgCl_2$-KCl is 35 times higher than the 15 microns per year target
- Non-isothermal corrosion for Haynes 230 with only free convection is over 100 times higher than the target

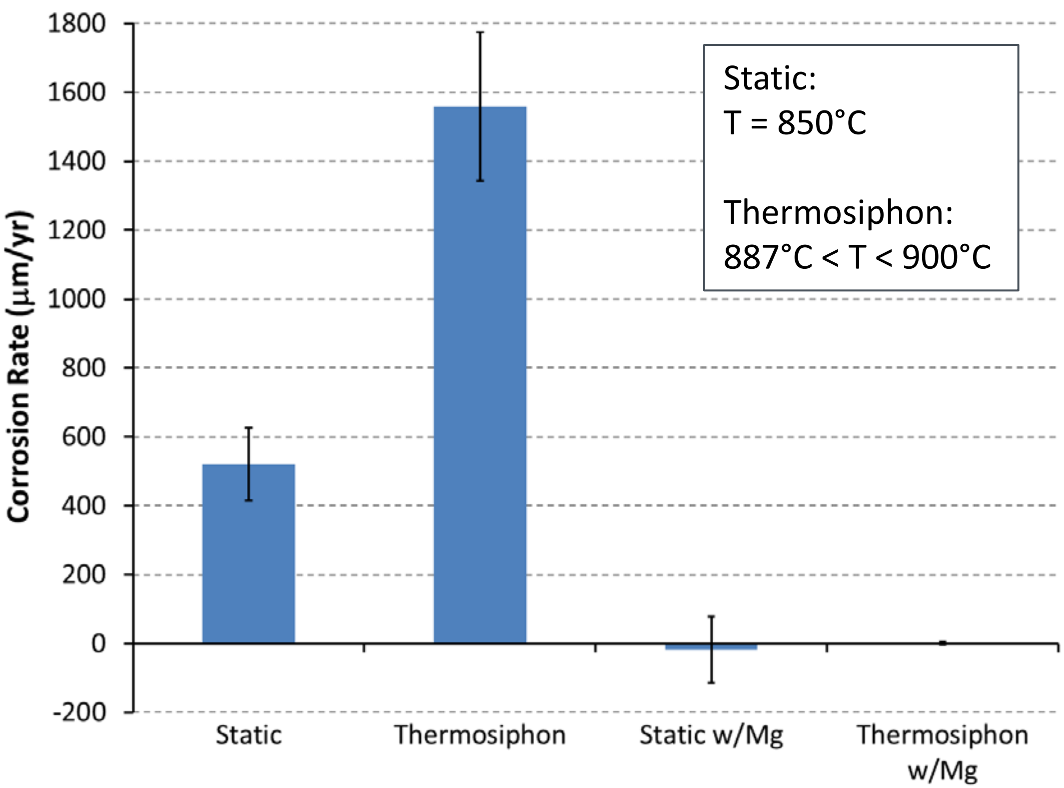

- Tests with Mg as a corrosion inhibitor species eliminated weight loss in the samples for static test
- An improved understanding of the long term behavior of systems with Mg corrosion inhibition is needed along with a method to reliably control the amount of Mg present in a system

Corrosion Inhibitor Studies
EDS Mapping of Haynes 230 with Mg in Chloride Salt

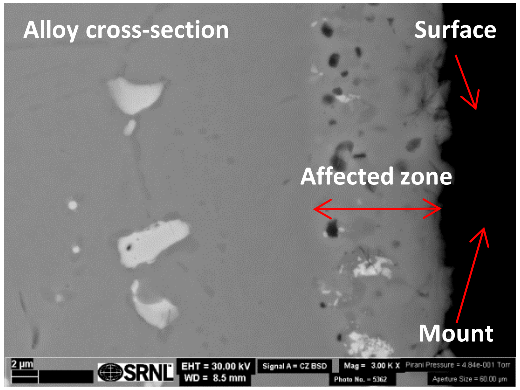

SEM of Cross-section

- **The SEM and EDS images for Mg used as a corrosion inhibitor in $MgCl_2$-KCl had an affected layer of about 5 microns thick**

EDS X-ray maps of cross-section

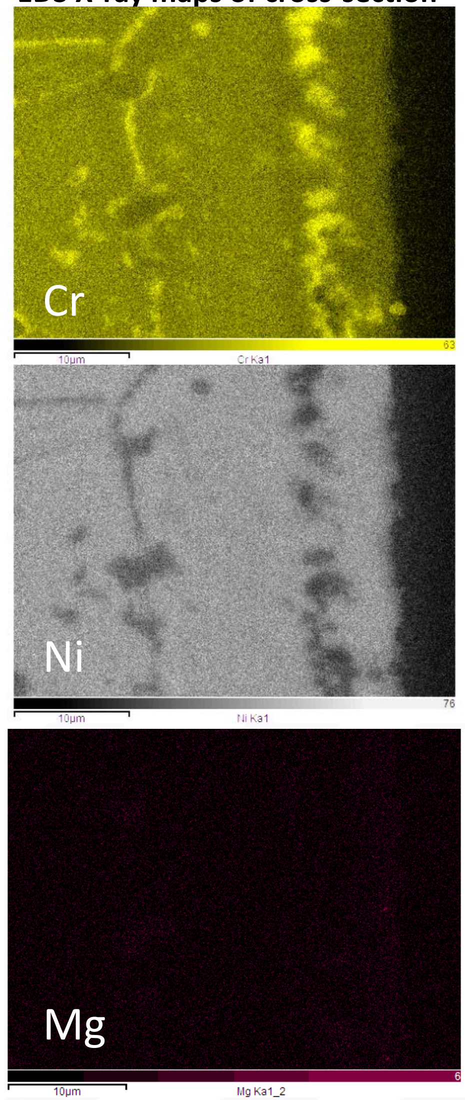

- There was a mild build up of chromium carbides about 5 microns beneath the surface
- The weight change in this sample was negligible
- The results indicate that Mg is effective at reducing corrosion in the samples with only minor changes in the sample microstructure

SEM Characterization of Welds

- Top weld of U-Bend samples examined under SEM for localized corrosion near weld interface → No localized corrosion observed for Haynes 230, Haynes NS-163, or Incoloy 800H
- Weld at top of U-bend coupon likely most susceptible to localized corrosion due to heat affected zone and constant imposed stress
- Aside from apparent change in secondary phase orientation from welding (stringers not aligned in Haynes 230 weld), EDS analysis of composition differences showed no significant differences

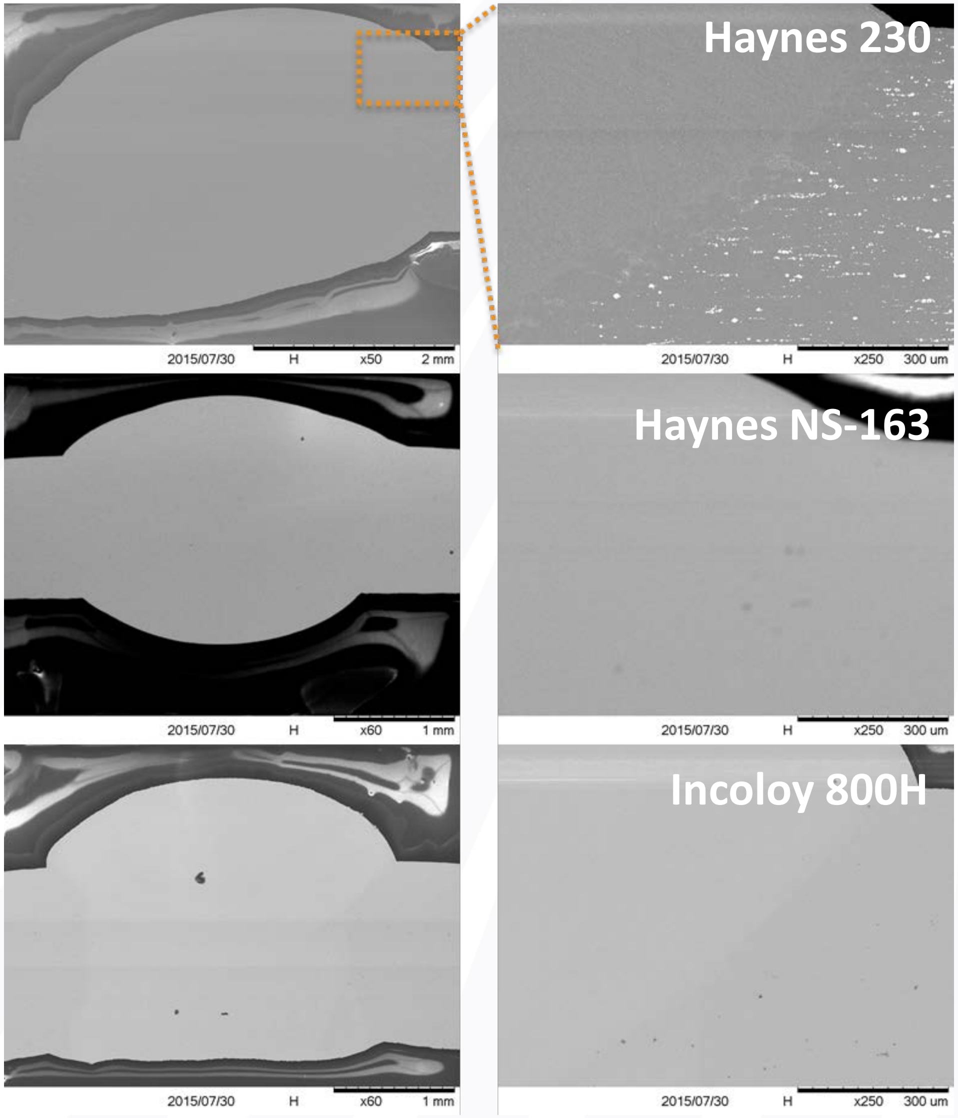

Conclusions

- The primary corrosion mechanism for high strength alloys in molten chloride salts is the selective oxidation of Cr
- The reaction mechanism for the selective oxidation of Cr is mass transfer limited and it has been shown that corrosion occurs significantly faster in systems with convective flow
- A mechanism to explain the corrosion of coupons in the nickel crucibles was developed to explain the observed corrosion phenomena and predicted the formation of a NiCr alloy at the crucible surface
- The thermodynamic inhibition of corrosion using Mg as an additive to the $MgCl_2$-KCl salt was demonstrated
- Corrosion potential monitoring experiments showed that the Mg addition to the salt lowered the corrosion potential for the coupons below the equilibrium potential for all of the alloy components and prevents their oxidation as expected
- The use of corrosion potential monitoring along with additions of Mg to the salt is a potential method to control corrosion in CSP systems
- Corrosion models have been developed and implemented in CFD software to describe the corrosion in the molten salt systems

Path to Market

- Developed software using CFD subroutines that can be licensed by system developers for analyzing corrosion rates in non-isothermal systems
- Prototype development in progress for a commercial reference electrode that can be used in molten salts that can help to identify locations that are susceptible to corrosion
- Developed concepts for process control to introduce corrosion inhibitors in CSP systems
- Consulting and collaborating with industrial partners such as Haynes International, ICL, and Solar Reserve to assist in corrosion control efforts